MPsizeBase: a database for particle size distributed environmental microplastic data

Jeroen E. Sonke^{1*}, Théo Segur^{1*}, Ian Hough², Nela Dobiasova², Didier Voisin², Nadiia Yakovenko^{1,3}, Henar Margenat⁴, Oskar Hagelskjaer^{3,4}, Sajjad Abbasi¹, Silvia Bucci⁵, Camille Richon⁶, Hélène Angot², Jennie L. Thomas², Gael Le Roux⁴

- ¹Géosciences Environnement Toulouse, CNRS, IRD, Université de Toulouse, 31400 Toulouse, France.
- ²Institut de Géosciences et de l'Environnement, Univ. Grenoble Alpes, CNRS, INRAE, IRD, Grenoble INP,
 Grenoble, France.
 - ³Microplastic Solution, 31320 Castanet-Tolosan, Toulouse, France.
- ⁴Centre de Recherche sur la Biodiversité et l'Environnement, CNRS, Toulouse INP, IRD, Université de Toulouse, France.
 - ⁵Department of Meteorology and Geophysics, University of Vienna, Vienna, Austria.
 - ⁶Laboratoire des sciences de l'Environnement Marin, CNRS, IRD, Ifremer, Université de Brest, Plouzané, France

*Corresponding authors: jeroen.sonke@cnrs.fr, theo.segur@get.omp.eu

Abstract

Understanding the sources, dispersion, and health impacts of microplastic (MP) pollution requires quantitative observations in terms of MP number and/or mass concentrations. Measurements of environmental MP fragments or fibers typically target variable size spans within the formal 1 to 5000 µm range, due to different sampling and detection techniques, and are therefore not directly comparable. In addition, the majority of measurements by microscopy techniques are number based, whereas life cycle analysis, numerical models for MP dispersion and policy evaluation, and plastic additive exposure estimates are mass based. Data analysis frameworks, based on measured MP particle number size distribution (PSD), have been developed to align and extrapolate measurements to a common MP size range (e.g. 1-5000 or 1-300 µm), which in turn allows direct data inter-comparison. In this study we present the MPsizeBase, a database of published MP number concentrations and PSD in the environment, including land, ocean and atmosphere. MPsizeBase uses the power law to fit observed MP cumulative number PSDs, and extrapolate and align observations over a common size range of choice. Assuming MP shape and volume approximations, MPsizeBase also estimates size-aligned MP mass concentrations. We illustrate how the MPsizeBase can be used for inter-comparison studies, and end with recommendations on MP size, shape, and PSD reporting, including length, width and surface area. We invite scientists to contribute old and new data to MPsizeBase for additional environmental compartments, including soils, sediment and biota.

Introduction

Recent unsustainable growth in plastic production, use and mismanaged waste is confronted with the ecological, social and health impacts it makes (Thompson et al., 2024). The petroleum and polymer industries are responsible for nearly 4% of modern global greenhouse gas emissions, a figure that may rise to 15% by 2050 (Zheng and Suh, 2019) under the anticipated redirection of petroleum resources from the transport to the polymer sector. The miracle properties of synthetic polymers such as plasticity and durability do not last, and degradation of plastic produces microplastic (MP) particles (Thompson et al., 2004). MP, from one micrometer to five millimeters in size, is now found in all Earth surface environments, from the highest mountains (Allen et al., 2021) to the deepest Ocean trenches (Peng et al., 2018). MP enters our food, and the air we breathe, reaching our internal tissues, from the brain to our reproductive organs (Hu et al., 2024; Nihart et al., 2025). In the environment and inside our body, plastics release toxic chemicals such as additives and monomers that disrupt endocrine function and increase risk for neurodevelopmental disorders, reproductive birth defects, infertility, cardiovascular disease, and cancers (Landrigan et al., 2023). In short, the unsustainable growth in plastic production and mismanaged waste has culminated in a plastic Ponzi scheme

because economic activities are distanced, spatially, temporally and socially from their environmental impacts (Sonke et al., 2025b). A globally-binding policy instrument to curb plastic pollution is currently under negotiation at the United Nations.

Over the past ten years numerous sampling and analysis protocols have been developed for MP identification and classification. Many of these are microscopy based, including manual microscopy, fluorescence microscopy after Red-Nile staining (Hidalgo-Ruz et al., 2012), Fourrier-transform infra-red (FTIR) and Raman micro-spectroscopy (Primpke et al., 2020). Microscopy techniques typically involve contrast-based digital image or spectral image analysis, resulting in statistical data on particle length and width, and a measure of MP 'number' concentrations expressed as MP counts per volume or per mass of sample matrix. In addition, FTIR and Raman micro-spectroscopy provide chemical identification of the polymer type, such as polyethylene, polystyrene etc. MP number concentrations can be converted to MP mass concentrations if the particle density and volume are known. Alternative techniques, such as pyrolysis-gas chromatography - mass spectrometry (pyGCMS) provide a direct measurement of polymer mass concentration, but do not provide information on particle size (Fischer and Scholz-Böttcher, 2019). Studies that do provide MP particle size statistics generally do so for different size ranges, making them difficult to compare. Standardized data intercomparison and inter-conversion methods, from number to mass concentrations and vice versa, are therefore needed to address MP pollution and exposure (Barchiesi et al., 2023; Kooi and Koelmans, 2019). MP mass concentrations, stocks and mass fluxes are for example needed for life cycle analysis of plastic and MP (OECD), for environmental plastic and MP dispersal budgets (Sonke et al., 2025a), for plastic additive exposure estimates (Trasande et al., 2024).

In this contribution we present the CNRS MPsizeBase, a database of peer-reviewed MP number concentrations and particle number size distributions (PSD) in the environment. By extending established particle size alignment approaches (Koelmans et al., 2020; Leusch et al., 2023), we illustrate how the measured PSD of individual studies can be used to extrapolate and intercompare MP concentration data. MPsizeBase currently contains ~50 studies with ~100 PSDs for common microplastic shapes (fragments, fibers, films) in aerosols, atmospheric deposition, surface ocean, and subsurface ocean. The MPsizeBase also contains key metadata on sample type, sampling methods, geographical location, and many additional parameters, providing a long-needed catalogue of knowledge gathered by and for the microplastics community. We briefly discuss data uncertainty, limitations of PSD-based MP concentration extrapolation, and end with recommendations on PSD data reporting. Ideally the database will be expanded to include all environmental media, including sediments, soils and biota amongst others. Scientists have access to MPsizeBase via the web portal (https://www.get.omp.eu/mpsizebase/) and via Zenodo (10.5281/zenodo.17380284), and can contribute new and published data via the web portal.

Particle size distribution and the power law

Intercomparing microscope-based MP number concentrations is challenging, because studies generally target different MP size ranges within the formal 1 to 5000 μ m range. The observed range is generally dictated by the methods' limit of detection (LOD) on the lower end, and by the sample volume and occurrence of less abundant larger MP on the higher end. In addition, studies tend to bin MP number observations using widely variable bin size ranges. Figure 1a,b illustrates an example where an imaginary (simulated) Raman 'study A' reports 888 MP_{10-90 μ m} m⁻³ of air in the 10-90 μ m range (10 μ m bin size range), and an FTIR 'study B' reports 34 MP_{250-1750 μ m} m⁻³ for the same sampling site in the larger 250-1750 μ m size range (250 μ m bin size range). Concluding that study A found higher MP concentrations than study B, at the same site, is potentially incorrect and symptomatic of comparing proverbial apples and oranges. Intercomparison of studies A and B must be done over identical size ranges.

An important starting point to intercompare MP studies is to examine the measured MP particle number size distribution (PSD), illustrated in Figure 1a,b for studies A and B as histograms on linear scales, and in Figure 1c on log scales. Observed particle number size distributions in nature have been commonly represented by a power law, $y = bx^a$ (Bader, 1970), with a<-1 which was first illustrated for marine MP (Cozar et al., 2014) and observed by many studies since then . In this formulation, y is the number of particles having length in the infinitesimal range x to x + dx. An important property of the power law is that its exponential behavior (Figure 1a,b) is linearized on log scales (log(y) = a*log(x)+log(b), Figure 1c,), so that intercept, b, and slope, a, can be obtained by linear regression. The slope reflects the relative abundance of

127

128

129

130

131

132 133 134

135

136

137

small vs. large particles, with steeper negative slopes corresponding to more small particles. The intercept reflects the total number of particles, with higher values corresponding to more particles.

Data analysis and alignment frameworks, based on power law fits of measured MP PSD, have been developed to extrapolate MP concentration measurements to identical MP size range (e.g. 1 to 5000 or 1-300 um), which in turn allows direct data inter-comparison (Koelmans et al., 2020; Kooi and Koelmans, 2019). Figure 1c illustrates that the individual PSD of studies A and B are both part of the same broader PSD once we normalize MP concentrations for (i.e. divide by) reported MP bin width (10 µm in A, 250 µm in B). In other words, both datasets can be fitted with the same power law equation $y = bx^a = 10,000x^{-2}$, where x is the representative MP length of a bin (estimated as the geometric mean of the bin boundaries in µm), and y is the bin-normalized MP number concentration (MP m⁻³ µm⁻¹). Now that we have fitted the bin-normalized BN-PSDs, we can extrapolate the observations of both studies A and B to the formal 1-5000 µm MP size range by integrating the surface area under the power law BN-PSDs in Figure 1c:

$$MP_{1-5000\mu m}^{\#} = \int_{1\mu m}^{5000\mu m} bx^a dx = \frac{b}{1+a} (5000^{1+a} - 1^{1+a})$$
 (Eq.1)

where b = 10,000, and a = -2. Doing so will return identical MP_{1-5000µm} concentrations of 9998 MP/m³ for both studies A and B. Reported PSDs are therefore critical in normalizing and extrapolating MP concentration data so that we can intercompare studies over any MP size range. In the case of our example, studies A and B sampled the same air, but observed different parts of the MP PSD, and are therefore highly complementary, delivering identical MP concentrations after alignment. Although beyond the scope of this contribution, understanding variability in PSDs, in particular the exponent a that typically varies between -1 and -3, informs us on plastic fragmentation mechanisms, and on natural particle sorting processes such as sedimentation, emission and deposition (Segur et al., 2025).

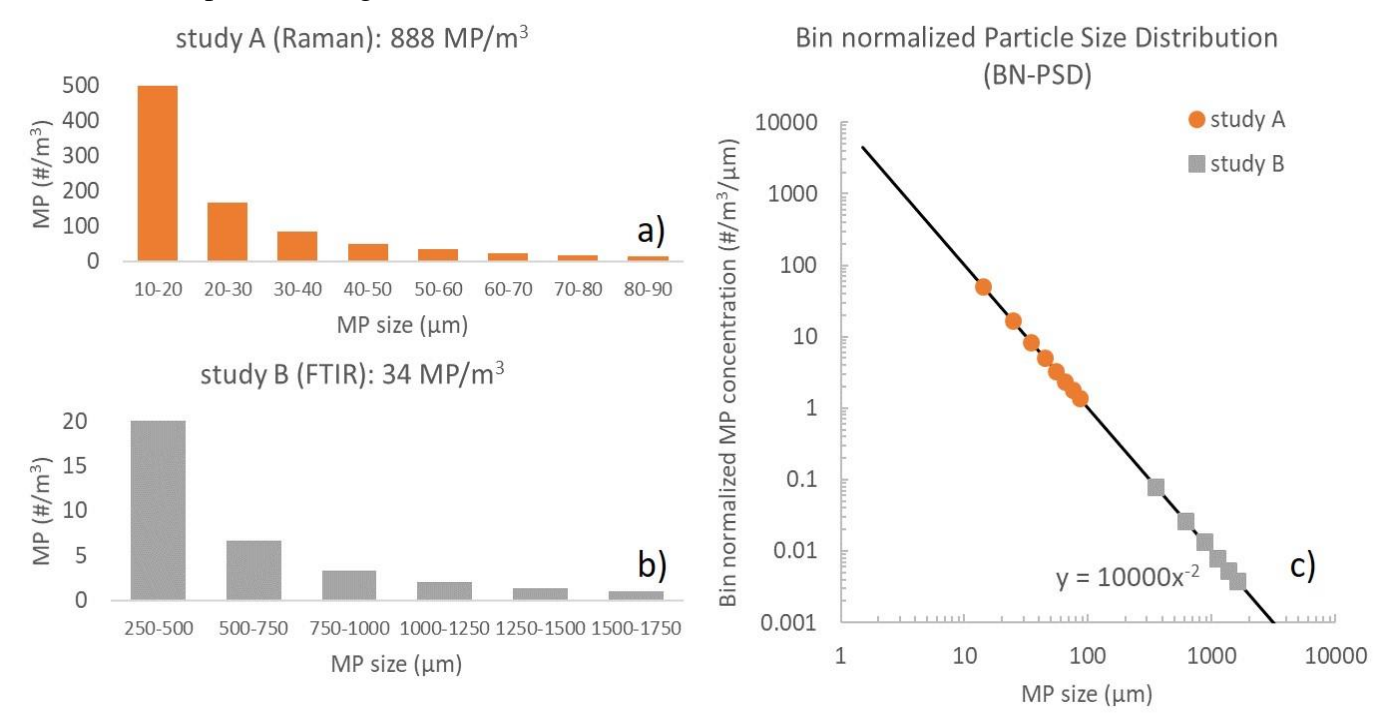


Figure 1a-c. Two hypothetical studies that observe MP number concentrations in air at the same site, but using different micro-spectroscopy techniques. a) Study A, using Raman, observes high a number concentration of small MP_{10-90um} (888 MP m⁻³). b) Study B, using FTIR, observes a lower number concentration of larger MP_{250-1750µm} (34 MP m⁻³). By normalizing the observed MP particle size distributions (PSD) in a and b to their respective bin size (10 and 250µm), we can see in c) that both studies define an identical bin-normalized BN-PSD, fitted with a power law as $y = 10,000x^{-2}$. Consequently, extrapolating the limited observed MP range, to the full, formal 1-5000 µm range (using Eq.1) aligns the observations and returns identical MP_{1-5000um} concentrations of 9998 MP m⁻³ for both studies A and B.

144

145

146

147

148

149

150

151

152

153

154

155

156

157

158

159

160

161

162

163

164

165

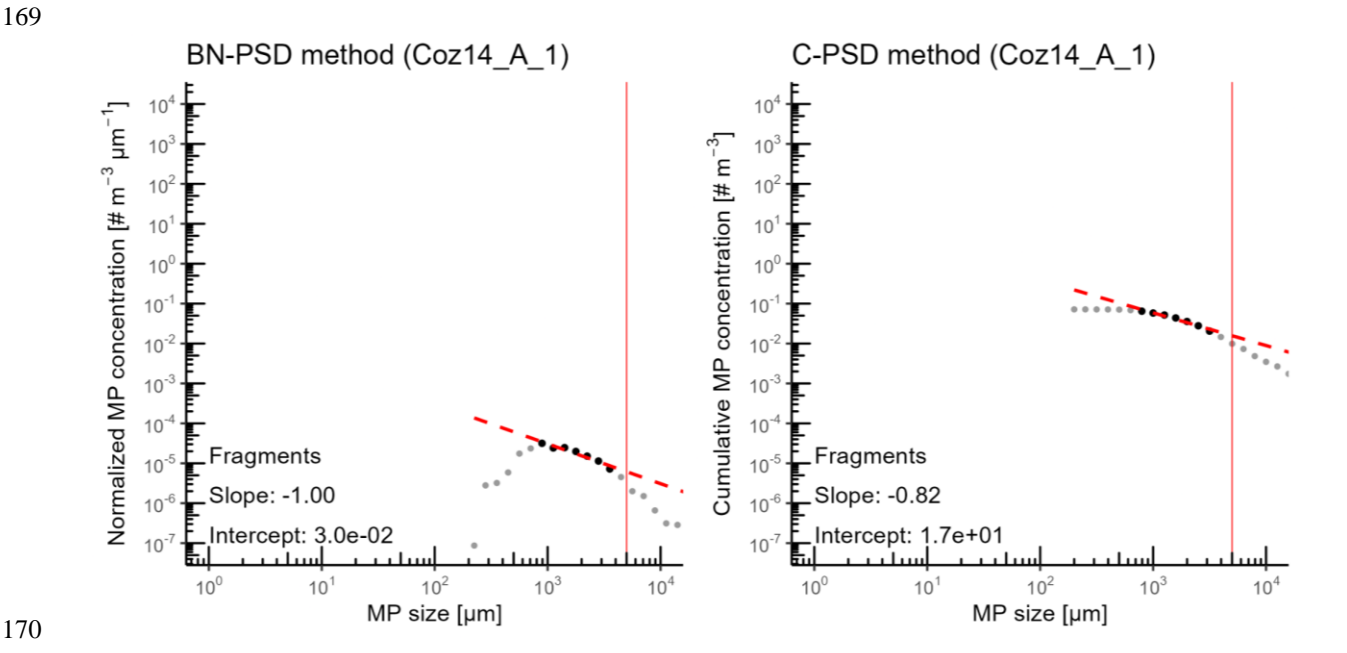
166

167

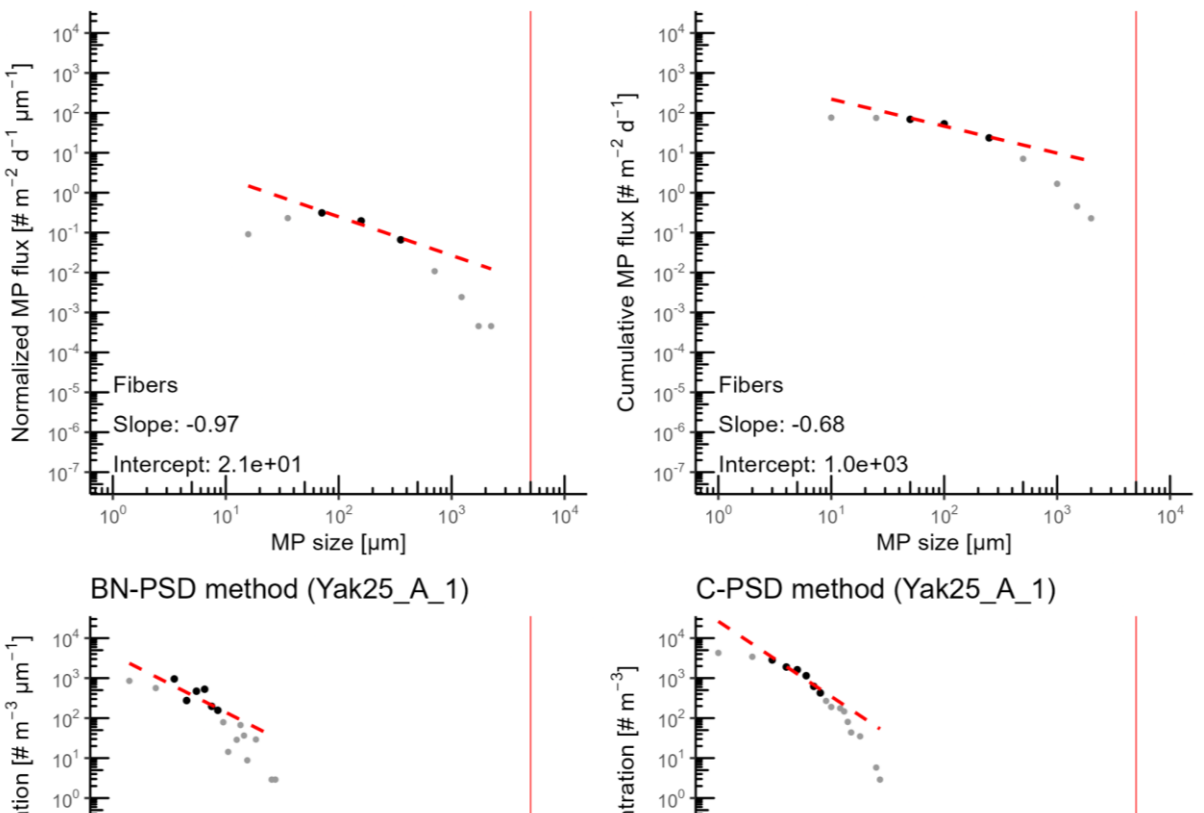
168

Real world, published MP PSD histograms do not behave like the ideal PSDs in the above example (Figure 1), and it has been observed that power law slope b, and intercept a depend directly on the chosen PSD bin size (Leusch et al., 2023; Segur et al., 2025). That is problematic because incorrect power law coefficients a and b lead to erroneous MP concentration extrapolation using Eq.1, undermining the entire data alignment method. Binning bias can technically be avoided by fitting raw MP number data (Kooi et al., 2021), yet very few studies have published such raw data and instead have published binned PSD histograms. In MPsizeBase we apply a practical solution to the binning bias problem by transforming the regular binned PSD to a complementary cumulative binned PSD (Segur et al., 2025; Virkar and Clauset, 2014). The cumulative PSD (C-PSD hereafter) gives the number of particles having length $\geq x$. It can be computed from a binned PSD by successively adding the bins' non-normalized MP number concentrations, starting with the bin containing the largest particles and proceeding to the bin containing the smallest particles. This results in a new log-log distribution that is linear for most of the PSD and is far less sensitive to bin width and binning bias (Segur et al., 2025). C-PSDs are shown in Figure 2 for three published datasets compiled in MPsizeBase, alongside their BN-PSDs. Log-log C-PSDs have three important properties (Segur et al., 2025): 1) the bin size, x is no longer represented by the geometric mean, but the lower bin limit, 2) the slope is shifted by +1 (less steep) compared to the original non-cumulative PSD or BN-PSD, and 3) the right tail of the C-PSD distribution, representing low counts for large MP, does not follow the power law, and therefore has to be omitted before fitting. A drop in the right tail also occurs for regular PSDs and BN-PSDs, and will be discussed below in the context of an upper limit of MP detection.

As mentioned, in log-log space, the C-PSD power law has a slope a' = a+1 (meaning the original BN-PSD slope is shifted by +1) and an intercept b' = -b/(a+1) (Segur et al., 2025). The parameters a and b are therefore computed from the slope a' and log-intercept, $log10^{(b')}$, obtained from linear regression of the C-PSD: a = a'-1 and b = -b'a'. The extrapolated MP number concentration within the size range 1 to 5000 μ m is again given by Eq.1 above. One can adjust the formal 1-5000 μ m size range in Eq.1 to any size range of choice.







Normalized MP concentration [# m⁻³ µm⁻¹] Cumulative MP concentration [# m⁻³] 10⁻ 10⁻² 10⁻⁴ 10⁻³ 10-10~ Fragments Fragments Slope: -1.88 Slope: -1.44 Intercept: 3.8e+03 Intercept: 2.6e+04 10⁴ MP size [µm] MP size [µm]

Figure 2a-f. Three published MP fragment particle size distributions (PSD) illustrating the bin-normalized particle size distribution (BN-PSD, left panels) and the complementary cumulative C-PSD (right panels. The three data sets illustrate common behavior for three different MP size ranges observed with three different techniques: Coz_A_1 from 225-550,000 µm by digital microscopy (Cozar et al., 2014), Bra_C_1 from 18-2250 µm by FTIR microscopy (Brahney et al., 2020), and Yak_A_1 from 2-28 µm by Raman microscopy (Yakovenko et al., 2025). Fitted data points are shown in black, and delimit the lower and upper LOD, with data excluded from fitting in grey, according to criteria in Table 1. The vertical red lines highlight the formal MP range from 1 to 5000 µm. BN-PSD power law slopes are generally lower due to binning bias, which is avoided in the C-PSD fits.

MPsizeBase data QAQC

171

172

173

174

175

176

177

178

179

180

181 182

183 184

185

186

187

188

189

190

191

192

193

194

The studies currently integrated into the CNRS MPsizeBase are all peer-reviewed studies from the recent scientific literature, covering sampling years from 2010 to 2023. Typically 2 to 3 reviewers, in addition to editors, have verified quality assurance and quality control (QA/QC) criteria. The majority of studies publish a single 'generic PSD' histogram for fibers and/or fragments that includes the MP counts of all measured samples. We combine this generic PSD with the mean or median MP number concentration at a given location to estimate the absolute MP number concentration for each observed particle size bin. MPsizeBase metadata contains a comment (column), where we cite the original figures, tables, or text that provided PSD and MP concentrations. MPsizeBase includes all originally reported data, except for '0' MP counts that were removed. When studies report MP numbers at different geographical locations, or for different time periods at the same location (seasonality for ex.), or as a function of ocean depth, then we try to retain this spatiotemporal

variability but repeatedly apply the same, single reported generic PSD to generate particle size distributed MP number concentrations. Reported MP number concentrations at multiple sites were often found to be non-normally distributed, and we therefore converted reported mean values to medians when necessary.

We included QAQC indicators, which are the number of MP counts included in the published PSD, and the approximate number of MP counts measured for each individual sample (filter). The former is often explicitly reported in the methods section or with the PSD, while the latter was calculated indirectly by multiplying the mean MP number concentration, the volume of sample taken and the % of filter analyzed. Statistical considerations indicate that at least 96 particles need to be measured in order to obtain a 10% uncertainty on a single parameter of study, i.e. particle size (Cowger et al., 2024). In practice, true MP counts per sample are often low, and therefore studies generally sum up all MP observations and report a single size distribution. We currently do not exclude studies with low MP counts and consider that database users can use the QAQC indicators and additional statistics to decide if bias occurs, and if outlier studies should be removed from further data analysis. Database users are welcome to explore different LOD definitions and QAQC indicators.

Lower and upper LOD considerations during C-PSD fitting

As mentioned above, the measured PSD range is generally dictated by a methods' limit of detection on the lower MP size end (lower LOD), and by the sample volume and occurrence of less abundant larger MP on the higher MP size end (upper LOD). Authors generally do not formally define their LODs and report all MP counts made in their PSD. This often generates lower than expected counts for the smaller PSD bins (lower LOD bias), and zero or low MP counts for upper size bins (upper LOD bias). We illustrate this in Figure 2 for three published PSDs acquired with three types of microscopy, stereo, FTIR and Raman, and over three corresponding size ranges. Both LOD phenomena are important in fitting a C-PSD, and will be discussed in the following.

Lower LOD bias, originally observed for nearly all surface ocean water net tow samples, has historically been explained by a loss mechanism for small MP, such as sinking, biological uptake, or selective transport (Cozar et al., 2014; Isobe et al., 2014). Recently, MP fragmentation models suggested that the smallest fragments are fewer because the "energy" required to produce small fragments is higher (Aoki and Furue, 2021). In parallel, analytical scientists increasingly recognize that the various microscopy techniques, including manual stereo or digital microscopy, and FTIR and Raman micro-spectroscopy, have LODs related to the physical principles of the technique, operator bias, and sample matrix complexity (Primpke et al., 2020). Manual, FTIR and Raman spectroscopy have approximate size LODs (i.e. the limit of accurately identifying all MP of a given size in a sample) of 50-500 µm, 10-50 µm, and 1-10 µm respectively. Figure 2b,d,f illustrates that lower LOD bias, i.e. the lower than expected MP counts in smaller bins, occurs across the entire MP size range and for all techniques. In particular, FTIR and Raman studies show that power law behavior of MP occurs across the full MP size range, sometimes down to the 1 µm lower limit. Similar to previous work (Kooi and Koelmans, 2019), we therefore define the lower LOD cut-off at the turning point of the BN-PSD (i.e. the maximum MP count; Figure 2b,d,f), and remove the biased low counts from fitting the corresponding C-PSD. Note that it is more difficult to assign a lower LOD cut-off point directly in the C-PSD, because the cumulative nature of the distribution removes the turning point of the BN-PSD.

Upper LOD bias, which is the deviation of large MP counts from power law behavior, manifests itself as noise, and a drop in counts in the righthand tail of a BN-PSD, and similarly as a drop in cumulative counts in the corresponding C-PSD. To a large extent the upper LOD of the BN-PSD and C-PSD is related to two factors: i. The sampling volume, the % of the sample (i.e. filter area) analyzed, and the associated probability of detecting 1 or more MP of large size. For example, if surface ocean MP particles of 4 to 5 mm are present at a concentration of 1 MP/m3, then a low volume 0.1 or 0.5 m³ pumped sample will not recover sufficient MP, thereby underestimating the true concentration. Such a lower than expected concentration causes the PSD tails to slump downward. Conversely, if a 1 m3 pumped or 100 m3 plankton net tow sample were analyzed, then 1 and 100 MP would be recovered, potentially producing an accurate MP count and concentration. If, however, the 1 MP from the 1 m3 sample ends up on a FTIR filter, but only 10% of the filter is analyzed, then again chances are high that the single MP will not be found, biasing the 4-5mm MP counts low. ii) The second factor that causes a drop in the right-hand tail of the C-PSD is related to the sum of all large particles that have not been counted. This type of upper LOD bias is stronger for MP particles with less steep PSD slopes such as fibers.

For fitting purposes, we assign the upper LOD to the first of a group of large MP datapoints that clearly deviates from power law behavior (straight line in log-log space) in the C-PSD. Often the upper LOD roughly corresponds to bins that contain <5% of the MP counts in a PSD. In Figure 2a,c,e the MP counts above the upper LOD clearly define a slumping tail in the C-PSD and are therefore removed from the fitted data. MPsizeBase contains a column with comments on how the lower and upper LODs were assigned. For datasets to be fitted and included in MPsizeBase, at least 3 bins must remain after LOD assignment. Table 1 summarizes the PSD data analysis and fitting pipe line for published datasets included in the MPsizeBase. Figure 3 gives an overview of the reported MP size range for all 50 PSDs and the assigned LODs.

Although there is today growing consensus that the full 1-5000 µm size range of MP obeys the power law (Kooi et al., 2021; Segur et al., 2025), there are numerous physical processes that induce environmental MP particle sorting (settling, emission, deposition), affecting the PSD shape and slope (Kaandorp et al., 2021). Hyperbolic PSD shape is in fact a common phenomena in geology (Bagnold and Barndorff-Nielsen, 1980), while atmospheric aerosols other than MP generally follow a multimodal size distribution represented as the combination of multiple log-normal distributions (Grythe et al., 2014). We alert MP scientists that our attribution of a lower LOD to fit only the quasi-linear part of the log-log C-PSD is in fact an argumented assumption. This assumption, that environmental MP PSDs follow a power law facilitates data alignment, yet we should, as a community, remain receptive to changes in this assumption and paradigm in the future.

Table 1. PSD data analysis and fitting pipe line for published datasets included in the CNRS MPsizeBase

| Tuble 1 | . I SD data analysis and fitting pipe line for published datasets included in the CNRS MI sizeBase | | | | | | | | | | |
|---------|--|--|--|--|--|--|--|--|--|--|--|
| Step | Action | | | | | | | | | | |
| 1 | Recover published MP number PSD from Figures (digitize) or Tables; recover MP number | | | | | | | | | | |
| | concentration, and metadata. Have the extracted data validated by a 2nd person. | | | | | | | | | | |
| 2 | Normalize (divide by) the published number PSD by bin size and visually examine the (bi | | | | | | | | | | |
| | normalized) BN-PSD to assign the lower LOD at the BN-PSD lefthand turning point (if any), i.e. | | | | | | | | | | |
| | the maximum MP abundance (%). | | | | | | | | | | |
| 3 | Convert the original, non-binned number PSD (not the BN-PSD) to a cumulative C-PSD and visually | | | | | | | | | | |
| | examine the righthand tail to assign the upper LOD. Three criteria are used: 1. All bins and data | | | | | | | | | | |
| | beyond the first 'zero' MP count are removed, 2. All bins and data beyond 5000 µm are removed, | | | | | | | | | | |
| | 3. Residual large bins with low MP counts (typically <5%) often generate a slumping tail in the C- | | | | | | | | | | |
| | PSD because MP are undercounted; the upper LOD can be assigned to the knickpoint or to bins with | | | | | | | | | | |
| | >5% of total counts ^a . | | | | | | | | | | |
| 4 | Fit the C-PSD on a log-log scale with the linearized power law for data points between the lower | | | | | | | | | | |
| | and upper LOD. Convert the C-PSD fitted slope a' and intercept b' to regular PSD slope a and | | | | | | | | | | |
| | intercept b : $a = a'-1$ and $b = -b'a'$. | | | | | | | | | | |
| 5 | Use the PSD fit parameters a and b to extrapolate, via Eq.1, the observed MP number concentration | | | | | | | | | | |
| | to any size range of interest, such as the formal MP _{1-5000μm} window. | | | | | | | | | | |
| 6 | Use a and b in Eqs. 5-7 to derive MP mass concentrations for the size range of interest. | | | | | | | | | | |
| | | | | | | | | | | | |

^aSome studies logically bin many low count large MP into a single wide bin, e.g. from 2000-5000um. This can lead to that single bin carrying >5% of MP counts, but still displaying 'a slumped tail'. Such bins are also excluded in the C-PSD fitting procedure.

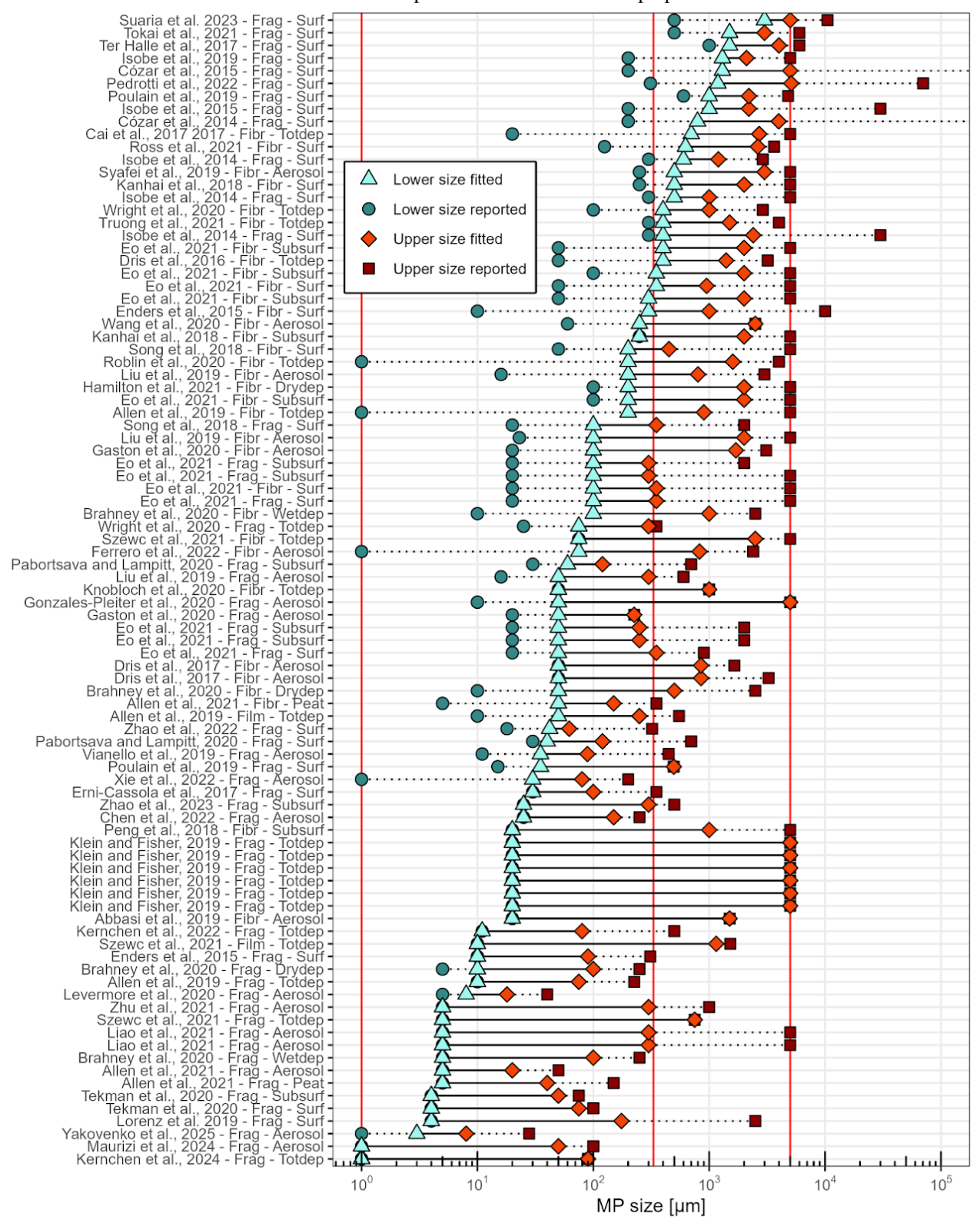


Figure 3. Size range reported by all studies currently compiled in MPsizeBase. The initial lower size marker (dark blue circle) is the minimum MP size reported by a study. The filtered lower size (light blue triangle) is the lower MP size used for power law fitting and represents the lower limit of detection (LOD), based on the highest MP concentration in the BN-PSD. The upper MP size reported is shown as brown squares, and the upper LOD fitted as red diamonds. Operational size ranges for small microplastics (SMP, 1 to 300 μ m), large microplastics (LMP, 300 to 5000 μ m) and meso and macroplastics (P, > 5000 μ m) are delimited by vertical red lines. LMP correspond approximately to the plankton/neuston net mesh for surface water MP sampling and the upper size range of MP fragments that can be emitted by oceans via the bubble bursting mechanism. The sample types are Surf (surface ocean waters), Subsurf (subsurface ocean waters) Aerosol (atmospheric MP) for studies reporting concentrations, and Totdep (Total deposition), Wetdep (Wet deposition), Drydep (Dry deposition) and Peat (Peat archive total deposition) for studies reporting atmospheric MP deposition.

MP number to mass conversion

Numerous studies in the literature convert MP number to MP mass concentrations by assuming an average MP weight, which is typically based on the measured average MP size. Because environmental MPs display a continuum of size and shape properties, MP volume and weight can vary by 11 orders of magnitude, from ~ 0.3 pg for the smallest 1 μm MP fragments, to ~ 10 mg for the largest 5000 μm MP fragments. Assuming an average MP weight, without taking into account the full PSD, therefore leads to very large uncertainties in MP mass concentration estimates, because both small and large MP are assigned the same average weight.

To convert a MP number concentration to a MP mass concentration, the particle density and volume need to be known for the measured MPs. Polymer density, ρ , varies relatively little (0.9 to $1.4 \times 10^{-6} \,\mu\text{g/}\mu\text{m}^3$) and is set here to $1 \times 10^{-6} \,\mu\text{g/}\mu\text{m}^3$ by default, but volume varies substantially according to particle shape and size. MPSizeBase includes observations of three common microplastic shapes: fragments, fibers, and films. Fragment MP volume depends on MP length, width (L, W, measured) and height (H, generally not measured). The majority of MP studies included in MPsizeBase unfortunately only reports L distributions (and not W). Dedicated MP morphological studies have observed that the median fragment W/L ratio is $0.67 \, +/- \, 0.03$, indicating an ellipsoid MP shape (Barchiesi et al., 2023; Contreras et al., 2024; Hagelskjær et al., 2025b; Kooi et al., 2021; Simon et al., 2018). It is often further assumed that ellipsoid H/W = W/L (Kooi and Koelmans, 2019; Simon et al., 2018), with a correction for surface irregularities based on the measured MP perimeter (Barchiesi et al., 2023). Recently, an ellipsoid volume model was calibrated for small MP and the special case when only L is known, and displayed $H/W = 0.40 \, +/- \, 0.08$ (Hagelskjær et al., 2025b). Therefore, in MPsizeBase, when MP fragment L is explicitly reported as the major MP axis, or major Feret diameter (L_{maj}), we approximate V based on the ellipsoid volume:

$$V_{ellipsoid} = \pi/6 \times L_{maj} \times W \times H = 0.094 \times (L_{maj})^{3}$$
 (Eq.2)

, where $W = 0.67 \times L_{maj}$ and $H = 0.40 \times W$. When fibers are reported, studies typically provide the PSD for fiber length, but rarely report the fiber diameter (*D*). If fiber *D* is not reported, we assume it to be 15 µm (Mintenig et al., 2020), which is a typical mean *D* measured in select studies (Wright et al., 2020). For fibers with L_{maj} shorter than 45 µm, we assume $D = L_{maj}/3$, in order to respect the common definition of fiber aspect ratio, L/W>3. Similar to previous studies we also assume environmental MP fibers to have a 40% void fraction (Barchiesi et al., 2023; Simon et al., 2018). MPsizeBase users are welcome to explore alternative volume and mass estimates in their studies. For MP film data we assume film thickness (*H*, height) to be 12.7 µm, which is the standard thickness of grocery bags, the most common littered film item. Fiber and film volume expressions in MPsizeBase are then defined as:

$$V_{fiber} = \pi \cdot (D/2)^2 \cdot Lmaj \cdot 0.6$$
 Eq.(3)

 $V_{film} = Lmaj \cdot W \cdot H$

Eq.(4)

, where for reported film data, W=L, and 0.6 refers to the non-void fraction of fibers. New studies reporting MP number PSDs are suggested to provide both L and W size distributions, or even better: single particle raw data in the Supporting Information, including L, W, area, and perimeter (and H, if at all possible). This will greatly aid in making more accurate MP count to mass conversions, which currently have a substantial uncertainty.

In MPsizeBase we estimate aligned, extrapolated MP mass concentrations by extending Eq.1 to include density and volume approximations (Eq.2-4), slope and intercept from the C-PSD fitting strategy, and then integrate:

fragments:

$$MP_{1-5000\mu m}^{mass} = \int_{1\mu m}^{5000\mu m} \rho. \, 0.094. \, x^3. \, bx^a dx = \rho. \, 0.094. \, \frac{b}{4+a} (5000^{4+a} - 1^{4+a})$$
 (Eq.5)

 $MP_{1-5000\mu m}^{mass} = \int_{1\mu m}^{5000\mu m} \rho.\pi. \, 0.6. \, (D/2)^2.x \, .bx^a dx = \rho.\pi. \, 0.6. \, (D/2)^2. \frac{b}{2+a} (5000^{2+a} - 1^{2+a}) (\text{Eq.6})$

$$MP_{1-5000\mu m}^{mass} = \int_{1\mu m}^{5000\mu m} \rho.H.x^2.bx^a dx = \rho.H.\frac{b}{3+a}(5000^{3+a} - 1^{3+a})$$
 (Eq.7)

341342

343

344

345

340

where $MP^{mass}_{1-5000\mu m}$ [µg m⁻³] is the MP mass concentration within the size range 1 to 5000 µm, ρ is the MP density of 1×10^{-6} µg/µm³, D is fiber diameter, H is film height, and a and b are the slope and intercept derived from C-PSD fitting. Note that we assume fibers have length $\geq 3 \text{xD}$ and films have length $\geq 10 \text{xH}$. Again, one can adjust the formal 1-5000 µm size range in Eqs.5-7 to any size range of choice.

346347

Data alignment uncertainty

348349

350

351

352

353

354

355

356

357

358

359

360

361

362

363

364

365

366

367

368

369

It is widely acknowledged by the MP community that concentration measurements are difficult to make, due to the wide variability and complexity of particles in the natural environment. Generally, MP are minority particles that need to be separated and pre-concentrated before identification is possible by microscopy. The many field and laboratory manipulations involved in this pre-concentration increase both the risk of contamination and MP loss. While most studies quantify and correct for contamination, procedural MP loss is rarely monitored, and standard operating procedures and certified reference materials remain under development (Hagelskjær et al., 2025a). Moreover, identification of MPs in natural samples often relies on comparison with libraries (FTIR, Raman, PyGCMS) which are incomplete and contain select polymers or additives only (Primpke et al., 2020; Santos et al., 2023). Multiple reference libraries exist and thus, two articles reporting MP counts or mass and polymer type may not have used the same libraries. The published MP data compiled in MPsizeBase, covering the period 2014-2023, therefore reflects this inherent measurement uncertainty, even before C-PSD data alignment. In MPsizeBase we estimate the standard error (SE) of C-PSD slope and intercept, and propagate those SEs during extrapolation from observed to expanded MP_{1-5000um} number and mass concentrations. Across all data, this leads to an average uncertainty of 100% on MP_{1-5000µm} number concentrations, and 55% on MP_{1-5000µm} mass concentrations. The reason for the difference is that MP numbers are dominated by the mostly unobserved 1-10 µm size range, requiring extrapolation and thus higher uncertainty, while MP mass is dominated by the typically observed 500-5000 size range, requiring less extrapolation. Alternative, more complex Monte Carlo based uncertainties can be evaluated by including or excluding additional data points in the C-PSD power law fit. We consider however that presently the largest contribution to the uncertainty of an aligned MP_{1-5000µm} concentration is not the C-PSD power law extrapolation, but the inherent methodological variability of the original measurements. By compiling as many datasets as possible, outlier data can be identified with standardized statistical tests among the aligned datasets.

370371372

373

374

Metadata

375376377

atmosphere, sediment, soil, biota,...), various subsample types (surface, subsurface, indoor, outdoor), and operational descriptors for fragments, fibers, films or pellets; Method details, including MP sampling, extraction and detection details, and sample ID; Geographical information (Figure 4), including latitude, longitude, altitude, continent, ocean basin, country, location, sampling dates; Ancillary parameters, such as population density etc. Scientists contributing new datasets can suggest columns with additional parameters.

The MPsizeBase includes different classes of metadata: Full reference and doi: General sample type (ocean,

379380

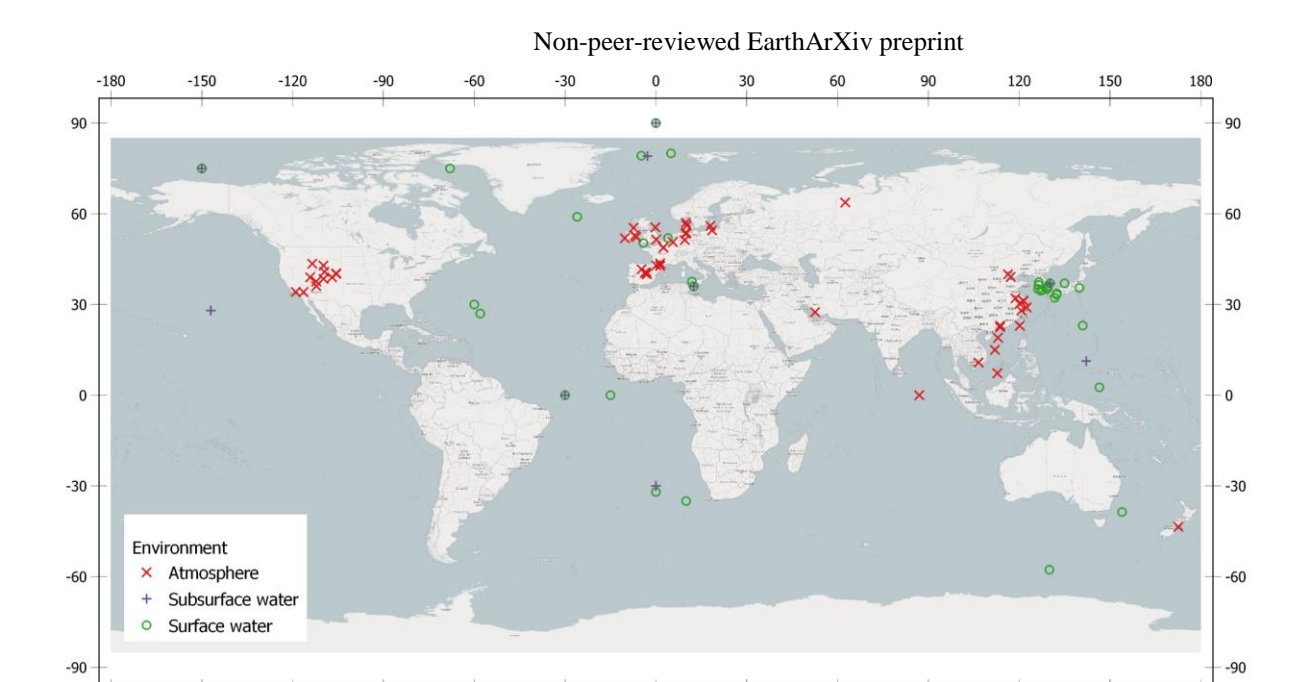


Figure 4. Map showing the geographical locations of ocean and atmosphere samples included in MPsizeBase v1.0. Ocean surface water includes the 0-50m deep surface mixed layer; ocean subsurface water refers to all samples below 50m depth. Because most studies pool all sample MP counts into a single PSD, much geographical MP concentration variability (e.g. an oceanographic cruise track) is assigned a single location, or grouped into 2-4 geographical zones.

Results and Discussion

 Supporting Information 1 (SI-1) provides a compact summary of all 50 MPsizeBase data sets, 100 individual PSDs, metadata, and extrapolated MP_{1-5000µm} number and mass concentrations. MPsizeBase users can adjust the standard 1-5000 µm extrapolation size range in SI-1 to integrate over a different size range. Alternatively, users can adjust the size range in the most up to date online version of MPsizeBase. Table 2 summarizes MP PSD properties, C-PSD fitting results and extrapolated MP_{1-5000µm} number and mass concentrations and atmospheric deposition fluxes for the major and sub-environmental MP categories in MPsizeBase (e.g. fibers, fragments, coastal, offshore, etc). Several key features are: 1. The systematically, 59x higher (median, n = 92 PSDs) extrapolated MP_{1-5000µm} number concentrations compared to the original reported observations for ocean and atmosphere. In general, the larger in size the observed MP number data are, the higher the extrapolation factor is, due to accounting for non-observed small MP. 2. The significantly higher fragment MP_{1-5000µm} number (39 000 MP m⁻³) and mass (6138 µg m⁻³) concentrations in coastal surface waters compared to offshore surface waters (223 MP m⁻³, 33 µg m⁻³). For fibers, this trend appears inverse but is not significant due to the small number of fiber MP concentration data points and PSDs. 3. The significantly different PSD slope between fibers (-1.39 ± 0.59) and fragments (-2.19 ± 0.67) in all major data groups, which partly reflects the dimensionality of fractal MP fragmentation (Segur et al., 2025).

Figure 5 visualizes measured atmospheric MP deposition fluxes in relation to extrapolated and aligned MP_{1-5000 μ m} fluxes for the formal 1-5000 μ m MP range. It illustrates how aligned MP_{1-5000 μ m} data are generally higher than the original MP measurements. Aligning different published MP measurements to the same MP range, whether it is 1-10, 1-300, 1-5000 μ m or other ranges, makes it possible to intercompare data sets, and compare observed MP concentrations to modeled MP concentrations.

The median PSD slopes for fibers and fragments reported in Table 2 can also be used to extrapolate and align MP number and mass concentrations for datasets without PSDs, following published methods (Koelmans et al., 2020). In addition, such generic PSD slopes (Table 2) can be used to align MP mass concentrations by thermo-analytical mass concentration measurements by pyGCMS provided that the analyzed MP size range is known from field and laboratory filtration procedures.



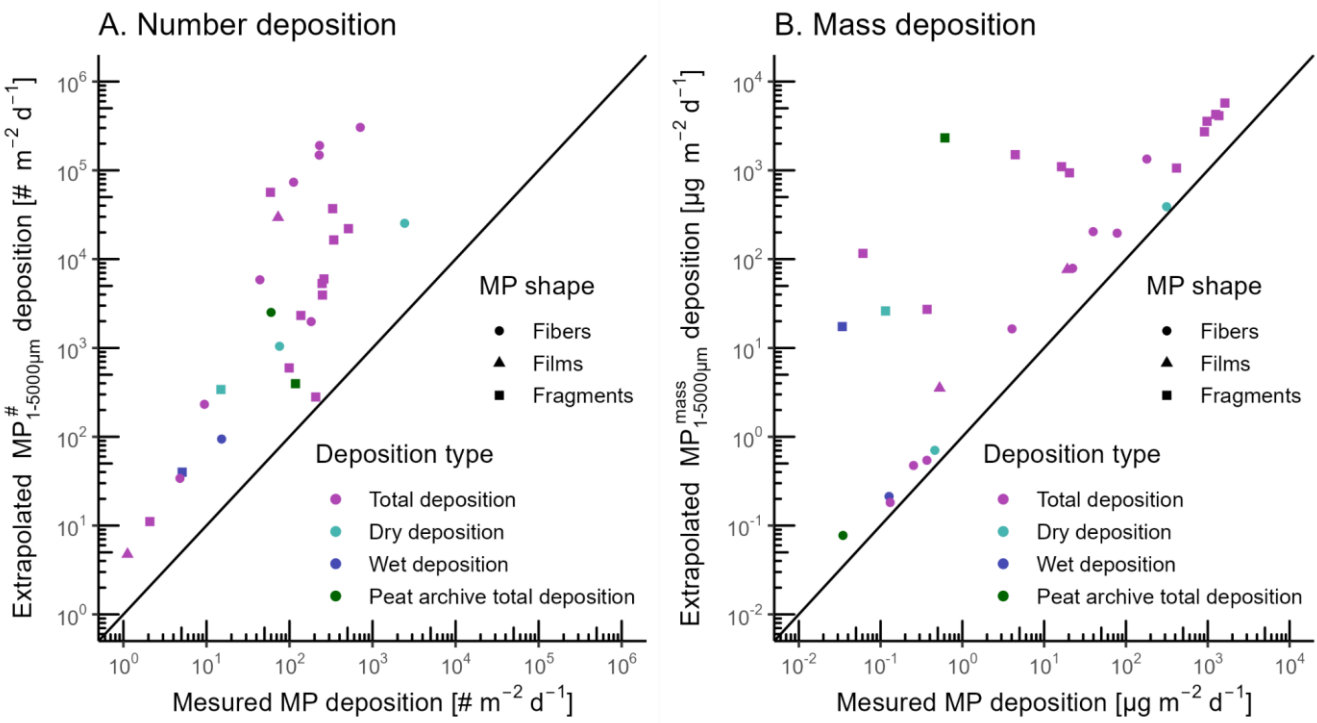


Figure 5. Comparison of measured atmospheric MP deposition fluxcto extrapolated MP_{1-5000µm} deposition flux in A. number (# m^{-2} y^{-1}) and B. mass (µg m^{-2} d^{-1}). Because only a fraction of the MP size spectrum between 1 and 5000 µm is measured, the extrapolated MP number and mass fluxes are generally higher.

Table 2. Summary of C-PSD data alignment for MP number and mass concentrations in surface ocean (coastal and offshore), deep ocean and atmosphere (aerosols, and total deposition, i.e. sum of wet and dry deposition). 'Coastal' corresponds to locations over the continental shelf (<140 m depth), n data points = number of samples or sites included, n PSD = number of particle size distributions across all data, rep = reported, est = estimated, # = number, IQR = interquartile range.

| | | | n | n | PSD | PSD | #MP/ | #MP/ | PS | D | MP# | MP# _{1-5000um} | | | MPmass _{1-5000um} | | |
|------------|----------|----------|--------|-----|--------|--------|--------|--------|-------|------|----------|-------------------------|-------|-----------|----------------------------|-------|--------|
| | | | data | PSD | min | max | PSD | sample | slope | | | | | | | | |
| | | | points | | | | | | | | | | | | | | |
| | | | | | rep | rep | rep | est | | | reported | estimated | | | estimated | | |
| | | | | | median | median | median | median | mean | SE | median | median | IQR | IQR | median | IQR | IQR |
| | | | # | # | μm | μm | # | # | | | #/m³ | #/m³ | | | μg/m³ | | |
| Ocean | | | | | | | | | | | | | | | | | |
| Surface | Fiber | Coastal | 12 | 4 | 100 | 3 500 | 118 | 12 | -1.85 | 0.20 | 195 | 5 443 | 3 749 | 9 376 | 28 | 17 | 45 |
| Surface | Fiber | Offshore | 4 | 3 | 250 | 3 500 | 117 | 4 | -1.92 | 0.28 | 48 | 180 456 | 4 145 | 397 104 | 61 | 0.5 | 135 |
| Surface | Fragment | Coastal | 17 | 10 | 143 | 3 175 | 346 | 87 | -2.14 | 0.12 | 123 | 39 066 | 1 922 | 1 140 543 | 6 138 | 507 | 37 972 |
| Surface | Fragment | Offshore | 16 | 12 | 225 | 4 825 | 528 | 4 | -2.15 | 0.11 | 0.03 | 223 | 17 | 811 | 33 | 5.0 | 450 |
| Deep | Fiber | | 14 | 7 | 125 | 3 500 | 82 | 4 | -1.97 | 0.18 | 42 | 16 422 | 212 | 40 748 | 22 | 4.2 | 78 |
| Deep | Fragment | | 18 | 8 | 35 | 1 000 | 459 | 33 | -2.48 | 0.16 | 163 | 46 187 | 6 216 | 83 245 | 1 605 | 1 103 | 2 653 |
| Atmospher | е | | | | | | | | | | | | | | | | |
| Aerosol | Fiber | | 10 | 8 | 85 | 2 632 | 96 | 7 | -1.80 | 0.09 | 1.0 | 10 | 5 | 77 | 0.049 | 0.008 | 0.055 |
| Aerosol | Fragment | | 17 | 9 | 18 | 213 | 508 | 35 | -2.25 | 0.21 | 26 | 461 | 86 | 1 416 | 686 | 74 | 2 557 |
| | | | | | | | | | | | #/m²/d | | | | μg/m²/d | | |
| Deposition | Fiber | | 34 | 12 | 110 | 3 100 | 186 | 21 | -1.82 | 0.09 | 41 | 1 273 | 611 | 5 549 | 0.55 | 0.26 | 6.1 |
| Deposition | Fragment | | 34 | 9 | 16 | 213 | 208 | 13 | -2.17 | 0.06 | 14 | 469 | 327 | 5 465 | 98 | 46 | 1 910 |

Reporting MP data in the literature

 Based on our experience in compiling MP observations, and developing the C-PSD data alignment framework, the following recommendations can be made for publication of MP number and PSD data:

- Provide raw MP particle size data in numerical format (.xls, .csv or other), as part of the supporting information or in an online data repository. Raw data, unbinned, provides the best estimate of MP number PSD slope and intercept (Kooi et al., 2021; Segur et al., 2025).
- Provide separate PSD's for MP fragments, fibers, films and other shapes (pellets, foams).
- If possible, report particle size data for each sampling location (provided the sample size is large enough)
- When observing fiber PSD, also report the mean/median fiber diameter, or better, the diameter size distribution. For MP films, the thickness would be of interest to measure and report.
- Provide, if possible, MP fragment length, width, area, perimeter and circularity measurements and PSDs (as raw data, and as binned histograms), which allows better estimates of height and volume, thereby limiting uncertainty of the number to mass concentration conversion (Barchiesi et al., 2023; Contreras et al., 2024; Hagelskjær et al., 2025b).
- Provide metadata in practical format, including latitude and longitude in decimals (not degrees)
- Scientists are welcome to use the provided MPsizeBase data template (SI) directly as Supporting Information with their own MP papers. This will facilitate rapid transfer to MPsizeBase and data use by the community.

In theory, a different PSD can be reported for every single sample, if sufficient MP counts are made to make that PSD robust. We recall that at least 96 particles need to be measured in order to obtain a 10% uncertainty on a single parameter of study, i.e. particle size (Cowger24). We recommend that if sufficient MP counts are made, it could be of great scientific interest to report raw data PSDs as a function of time, location, water depth, soil depth etc, in order to understand how physico-chemical processes sort and fractionate MP size, and where and how MP fragmentation takes place. An example of detailed raw data PSD analysis and slope variability in the aquatic environment can be found in Kooi et al. (2021). We emphasize that binning raw data leads to information loss on PSD and on MP size sorting (i.e. changes in PSD) to the point that we do not detect significant differences in PSD slope between aerosols, atmospheric deposition, surface ocean, and subsurface ocean. Understanding size sorting of MP in the environment is key because it controls both plastic mass transport of large MP, and biota exposure and uptake of small MP. Ideally, over the next decade the MP community consistently publishes raw PSD data, so that we can collectively tap into the full information contained within PSDs, and test data alignment frameworks that go beyond the power law.

Most spectroscopy or pyGCMS studies report MP polymer identity, which is a parameter that is under development in MPsizeBase, and therefore not discussed in detail here. In principle, if spectral polymer identification is accurate, there should be little intercomparison issues to be expected between FTIR, Raman or pyGC-MS. In reality, spectral identification by comparison to a spectral library is fraught with uncertainty. Incorrect assignment of measured particles as MP polymers directly leads to overestimation of MP number and mass concentrations. Expert spectroscopists are welcome to help add polymer identity to MPsizeBase, explore the associated uncertainty aspects, and explore potential relationships between polymer identity, PSDs and metadata.

Database use

Users will have open access to the latest validated version of the MPsizeBase here: https://www.get.omp.eu/mpsizebase/ and Zenodo (10.5281/zenodo.17380284). Users are asked to cite this publication and the doi associated with the version of the database; this in turn helps us secure the funding necessary to expand and maintain the database. Users can submit previously published and new peer-reviewed binned PSDs and raw PSDs on the MPsizeBase website. Users can also become active members of the MPsizeBase development group, and propose new approaches, concepts or parameters to include and explore.

Acknowledgements

- We acknowledge financial support from the CNRS, from the ANR-20-CE34-0014 ATMO-PLASTIC and
- 488 ANR-23-CE34-0012 BUBBLEPLAST grants, and from the French ministry of higher education. This project
- has received funding from the European Union's Horizon Europe research and innovation program under the
 - Marie Sklodowska-Curie Grant Agreement No. 101153990.

491492 **References**

490

493

494

495

496

503

505

508

510

515

- Allen, S., Allen, D., Baladima, F., Phoenix, V. R., Thomas, J. L., Le Roux, G., and Sonke, J. E.: Evidence of free troposp Allen,
- S., Allen, D., Baladima, F., Phoenix, V. R., Thomas, J. L., Le Roux, G., and Sonke, J. E.: Evidence of free
- tropospheric and long-range transport of microplastic at Pic du Midi Observatory, Nature Communications,
- 497 12, 7242, https://doi.org/10.1038/s41467-021-27454-7, 2021.
- 498 Aoki, K. and Furue, R.: A model for the size distribution of marine microplastics: A statistical mechanics
- approach, PLOS ONE, 16, e0259781, https://doi.org/10.1371/journal.pone.0259781, 2021.
- Bader, H.: The hyperbolic distribution of particle sizes, Journal of Geophysical Research (1896-1977), 75,
- 501 2822–2830, https://doi.org/10.1029/JC075i015p02822, 1970.
- Bagnold, R. A. and Barndorff-Nielsen, O.: The pattern of natural size distributions, Sedimentology, 27, 199–
 - 207, https://doi.org/10.1111/j.1365-3091.1980.tb01170.x, 1980.
- Barchiesi, M., Kooi, M., and Koelmans, A. A.: Adding Depth to Microplastics, Environ. Sci. Technol., 57,
 - 14015–14023, https://doi.org/10.1021/acs.est.3c03620, 2023.
- Brahney, J., Hallerud Margaret, Heim Eric, Hahnenberger Maura, and Sukumaran Suja: Plastic rain in
- protected areas of the United States, Science, 368, 1257–1260, https://doi.org/10.1126/science.aaz5819,
 - 2020.
- 509 Contreras, L., Edo, C., and Rosal, R.: Mass concentration of plastic particles from two-dimensional images,
 - Science of The Total Environment, 946, 173849, https://doi.org/10.1016/j.scitotenv.2024.173849, 2024.
- Cowger, W., Markley, L. A. T., Moore, S., Gray, A. B., Upadhyay, K., and Koelmans, A. A.: How many
- microplastics do you need to (sub)sample?, Ecotoxicology and Environmental Safety, 275, 116243,
- 513 https://doi.org/10.1016/j.ecoenv.2024.116243, 2024.
- Cozar, A., Echevarria, F., Ignacio Gonzalez-Gordillo, J., Irigoien, X., Ubeda, B., Hernandez-Leon, S.,
 - Palma, A. T., Navarro, S., Garcia-de-Lomas, J., Ruiz, A., Fernandez-de-Puelles, M. L., and Duarte, C. M.:
 - Plastic debris in the open ocean, PROCEEDINGS OF THE NATIONAL ACADEMY OF SCIENCES OF
- THE UNITED STATES OF AMERICA, 111, 10239–10244, https://doi.org/10.1073/pnas.1314705111,
- 518 2014.
- Fischer, M. and Scholz-Böttcher, B. M.: Microplastics analysis in environmental samples recent pyrolysis-
- 520 gas chromatography-mass spectrometry method improvements to increase the reliability of mass-related
- data, Anal. Methods, 11, 2489–2497, https://doi.org/10.1039/C9AY00600A, 2019.
- 522 Grythe, H., Ström, J., Krejci, R., Quinn, P., and Stohl, A.: A review of sea-spray aerosol source functions
- using a large global set of sea salt aerosol concentration measurements, Atmospheric Chemistry and Physics,
- 524 14, 1277–1297, https://doi.org/10.5194/acp-14-1277-2014, 2014.
- Hagelskjær, O., Hagelskjær, F., Margenat, H., Sonke, J. E., and Roux, G. L.: EasyMP: Diverse and
- 526 Environmentally Relevant Microplastic Reference Materials Encompassing Fragments and Fibers, Nano
- 527 Select, 6, e70004, https://doi.org/10.1002/nano.70004, 2025a.
- Hagelskjær, O., Margenat, H., Yakovenko, N., Le Roux, G., and Sonke, J. E.: Improving microspectroscopic
- microplastic data extrapolation: from field of view to full sample, and from fragment 2D-morphology to
- mass, Preprints, https://www.preprints.org/manuscript/202507.1300, 2025b.

- Hidalgo-Ruz, V., Gutow, L., Thompson, R. C., and Thiel, M.: Microplastics in the Marine Environment: A
- Review of the Methods Used for Identification and Quantification, ENVIRONMENTAL SCIENCE &
- 533 TECHNOLOGY, 46, 3060–3075, https://doi.org/10.1021/es2031505, 2012.
- Hu, C. J., Garcia, M. A., Nihart, A., Liu, R., Yin, L., Adolphi, N., Gallego, D. F., Kang, H., Campen, M. J.,
- and Yu, X.: Microplastic presence in dog and human testis and its potential association with sperm count
- and weights of testis and epididymis, Toxicological Sciences, kfae060,
- 537 https://doi.org/10.1093/toxsci/kfae060, 2024.
- Isobe, A., Kubo, K., Tamura, Y., Kako, S., Nakashima, E., and Fujii, N.: Selective transport of microplastics
- and mesoplastics by drifting in coastal waters, Marine Pollution Bulletin, 89, 324–330,
- 540 https://doi.org/10.1016/j.marpolbul.2014.09.041, 2014.
- Kaandorp, M. L. A., Dijkstra, H. A., and van Sebille, E.: Modelling size distributions of marine plastics
- under the influence of continuous cascading fragmentation, Environmental Research Letters, 16, 054075,
- 543 https://doi.org/10.1088/1748-9326/abe9ea, 2021.
- Koelmans, A. A., Redondo-Hasselerharm, P. E., Mohamed Nor, N. H., and Kooi, M.: Solving the
 - Nonalignment of Methods and Approaches Used in Microplastic Research to Consistently Characterize
- Risk, Environ. Sci. Technol., 54, 12307–12315, https://doi.org/10.1021/acs.est.0c02982, 2020.
- Kooi, M. and Koelmans, A. A.: Simplifying Microplastic via Continuous Probability Distributions for Size,
- Shape, and Density, Environ. Sci. Technol. Lett., 6, 551–557, https://doi.org/10.1021/acs.estlett.9b00379,
- 549 2019.

545

- Kooi, M., Primpke, S., Mintenig, S. M., Lorenz, C., Gerdts, G., and Koelmans, A. A.: Characterizing the
- multidimensionality of microplastics across environmental compartments, Water Research, 202, 117429,
- 552 https://doi.org/10.1016/j.watres.2021.117429, 2021.
- Landrigan, P. J., Raps, H., Cropper, M., Bald, C., Brunner, M., Canonizado, E. M., Charles, D., Chiles, T.
- 554 C., Donohue, M. J., Enck, J., Fenichel, P., Fleming, L. E., Ferrier-Pages, C., Fordham, R., Gozt, A., Griffin,
 - C., Hahn, M. E., Haryanto, B., Hixson, R., Ianelli, H., James, B. D., Kumar, P., Laborde, A., Law, K. L.,
- Martin, K., Mu, J., Mulders, Y., Mustapha, A., Niu, J., Pahl, S., Park, Y., Pedrotti, M.-L., Pitt, J. A.,
- Ruchirawat, M., Seewoo, B. J., Spring, M., Stegeman, J. J., Suk, W., Symeonides, C., Takada, H.,
- Thompson, R. C., Vicini, A., Wang, Z., Whitman, E., Wirth, D., Wolff, M., Yousuf, A. K., and Dunlop, S.:
- The Minderoo-Monaco Commission on Plastics and Human Health, Annals of Global Health,
- 560 https://doi.org/10.5334/aogh.4056, 2023.
- Leusch, F. DL., Lu, H.-C., Perera, K., Neale, P. A., and Ziajahromi, S.: Analysis of the literature shows a
- remarkably consistent relationship between size and abundance of microplastics across different
- environmental matrices, Environmental Pollution, 319, 120984,
- 564 https://doi.org/10.1016/j.envpol.2022.120984, 2023.
- Mintenig, S. M., Kooi, M., Erich, M. W., Primpke, S., Redondo-Hasselerharm, P. E., Dekker, S. C.,
- Koelmans, A. A., and van Wezel, A. P.: A systems approach to understand microplastic occurrence and
- variability in Dutch riverine surface waters, Water Research, 176, 115723,
- 568 https://doi.org/10.1016/j.watres.2020.115723, 2020.
- Nihart, A. J., Garcia, M. A., El Hayek, E., Liu, R., Olewine, M., Kingston, J. D., Castillo, E. F., Gullapalli,
- R. R., Howard, T., Bleske, B., Scott, J., Gonzalez-Estrella, J., Gross, J. M., Spilde, M., Adolphi, N. L.,
- Gallego, D. F., Jarrell, H. S., Dvorscak, G., Zuluaga-Ruiz, M. E., West, A. B., and Campen, M. J.:
- Bioaccumulation of microplastics in decedent human brains, Nature Medicine, 31, 1114–1119,
- 573 https://doi.org/10.1038/s41591-024-03453-1, 2025.

- Peng, X., Chen, M., Chen, S., Dasgupta, S., Xu, H., Ta, K., Du, M., Li, J., Guo, Z., and Bai, S.:
- 575 Microplastics contaminate the deepest part of the world's ocean, GEOCHEMICAL PERSPECTIVES
- 576 LETTERS, 9, 1–5, https://doi.org/10.7185/geochemlet.1829, 2018.
- 577 Primpke, S., Christiansen, S. H., Cowger, W., De Frond, H., Deshpande, A., Fischer, M., Holland, E. B.,
- Meyns, M., O'Donnell, B. A., Ossmann, B. E., Pittroff, M., Sarau, G., Scholz-Böttcher, B. M., and Wiggin,
- 579 K. J.: Critical Assessment of Analytical Methods for the Harmonized and Cost-Efficient Analysis of
- 580 Microplastics, Appl Spectrosc, 74, 1012–1047, https://doi.org/10.1177/0003702820921465, 2020.
- Santos, L. H. M. L. M., Insa, S., Arxé, M., Buttiglieri, G., Rodríguez-Mozaz, S., and Barceló, D.: Analysis
- of microplastics in the environment: Identification and quantification of trace levels of common types of
 - plastic polymers using pyrolysis-GC/MS, MethodsX, 10, 102143,
- 584 https://doi.org/10.1016/j.mex.2023.102143, 2023.

583

- Segur, T., Hough, I., Dobiasova, N., Voisin, D., Angot, H., Thomas, J. L., and Sonke, J. E.: Using the power
- law size distribution to extrapolate and compare microplastic number and mass concentrations in
- environmental media, In preparation, 2025.
- 588 Simon, M., van Alst, N., and Vollertsen, J.: Quantification of microplastic mass and removal rates at
- wastewater treatment plants applying Focal Plane Array (FPA)-based Fourier Transform Infrared (FT-IR)
- imaging, Water Research, 142, 1–9, https://doi.org/10.1016/j.watres.2018.05.019, 2018.
- Sonke, J. E., Koenig, A., Segur, T., and Yakovenko, N.: Global environmental plastic dispersal under OECD
- 592 policy scenarios toward 2060, Science Advances, 11, https://doi.org/10.1126/sciadv.adu2396, 2025a.
- Sonke, J. E., Segur, T., and Bucci, S.: Plastic Ponzi scheme, npj Emerging Contaminants, 1, 4,
- 594 https://doi.org/10.1038/s44454-025-00006-0, 2025b.
- Thompson, R. C., Olsen, Y., Mitchell, R. P., Davis, A., Rowland, S. J., John, A. W. G., McGonigle, D., and
- Russell, A. E.: Lost at Sea: Where Is All the Plastic?, Science, 304, 838–838,
- 597 https://doi.org/10.1126/science.1094559, 2004.
- Thompson, R. C., Courtene-Jones, W., Boucher, J., Pahl, S., Raubenheimer, K., and Koelmans, A. A.:
- Twenty years of microplastic pollution research—what have we learned?, Science, 386, eadl2746,
- 600 https://doi.org/10.1126/science.adl2746, 2024.
- Trasande, L., Krithivasan, R., Park, K., Obsekov, V., and Belliveau, M.: Chemicals Used in Plastic
 - Materials: An Estimate of the Attributable Disease Burden and Costs in the United States, Journal of the
- Endocrine Society, 8, bvad163, https://doi.org/10.1210/jendso/bvad163, 2024.
- Virkar, Y. and Clauset, A.: POWER-LAW DISTRIBUTIONS IN BINNED EMPIRICAL DATA, The
- Annals of Applied Statistics, 8, 89–119, 2014.
- Wright, S. L., Ulke, J., Font, A., Chan, K. L. A., and Kelly, F. J.: Atmospheric microplastic deposition in an
- urban environment and an evaluation of transport, Environment International, 136, 105411,
- 608 https://doi.org/10.1016/j.envint.2019.105411, 2020.
- Yakovenko, N., Pérez-Serrano, L., Segur, T., Hagelskjaer, O., Margenat, H., Le Roux, G., and Sonke, J. E.:
- Human exposure to PM10 microplastics in indoor air, PLOS ONE, 20, 1–15,
- 611 https://doi.org/10.1371/journal.pone.0328011, 2025.
- Zheng, J. and Suh, S.: Strategies to reduce the global carbon footprint of plastics, Nature Climate Change, 9,
- 613 374–378, https://doi.org/10.1038/s41558-019-0459-z, 2019.
- heric and long-range transport of microplastic at Pic du Midi Observatory, Nature Communications, 12, 7242,
- 615 https://doi.org/10.1038/s41467-021-27454-7, 2021.

- 616 Campen, M., Nihart, A., and Garcia, M.: Bioaccumulation of Microplastics in Decedent Human Brains
- Assessed by Pyrolysis Gas Chromatography-Mass Spectrometry, Research Square Preprint, 2024.
- 618 Cozar, A., Echevarria, F., Ignacio Gonzalez-Gordillo, J., Irigoien, X., Ubeda, B., Hernandez-Leon, S., Palma,
- A. T., Navarro, S., Garcia-de-Lomas, J., Ruiz, A., Fernandez-de-Puelles, M. L., and Duarte, C. M.: Plastic
- debris in the open ocean, PROCEEDINGS OF THE NATIONAL ACADEMY OF SCIENCES OF THE
- 621 UNITED STATES OF AMERICA, 111, 10239–10244, https://doi.org/10.1073/pnas.1314705111, 2014.
- Hu, C. J., Garcia, M. A., Nihart, A., Liu, R., Yin, L., Adolphi, N., Gallego, D. F., Kang, H., Campen, M. J.,
 - and Yu, X.: Microplastic presence in dog and human testis and its potential association with sperm count and
- 624 weights of testis and epididymis, Toxicological Sciences, 200, 235–240,
- 625 https://doi.org/10.1093/toxsci/kfae060, 2024.
- Landrigan, P. J., Raps, H., Cropper, M., Bald, C., Brunner, M., Canonizado, E. M., Charles, D., Chiles, T. C.,
- Donohue, M. J., Enck, J., Fenichel, P., Fleming, L. E., Ferrier-Pages, C., Fordham, R., Gozt, A., Griffin, C.,
- Hahn, M. E., Haryanto, B., Hixson, R., Ianelli, H., James, B. D., Kumar, P., Laborde, A., Law, K. L., Martin,
- K., Mu, J., Mulders, Y., Mustapha, A., Niu, J., Pahl, S., Park, Y., Pedrotti, M.-L., Pitt, J. A., Ruchirawat, M.,
 - Seewoo, B. J., Spring, M., Stegeman, J. J., Suk, W., Symeonides, C., Takada, H., Thompson, R. C., Vicini,
 - A., Wang, Z., Whitman, E., Wirth, D., Wolff, M., Yousuf, A. K., and Dunlop, S.: The Minderoo-Monaco
- 632 Commission on Plastics and Human Health, Annals of Global Health, https://doi.org/10.5334/aogh.4056,
- 633 2023.

623

630

631

635

- Peng, X., Chen, M., Chen, S., Dasgupta, S., Xu, H., Ta, K., Du, M., Li, J., Guo, Z., and Bai, S.: Microplastics
 - contaminate the deepest part of the world's ocean, GEOCHEMICAL PERSPECTIVES LETTERS, 9, 1-5,
- 636 https://doi.org/10.7185/geochemlet.1829, 2018.
- Thompson, R. C., Olsen, Y., Mitchell, R. P., Davis, A., Rowland, S. J., John, A. W. G., McGonigle, D., and
- Russell, A. E.: Lost at Sea: Where Is All the Plastic?, Science, 304, 838-838,
- 639 https://doi.org/10.1126/science.1094559, 2004.
- Thompson, R. S., Courtene-Jones, W., Boucher, J., Pahl, S., Raubenheimer, K., and Koelmans, A. A.: Twenty
- years of microplastics pollution research—what have we learned?, Science, 2024.
- Wilkinson, M. D., Dumontier, M., Aalbersberg, Ij. J., Appleton, G., Axton, M., Baak, A., Blomberg, N.,
- Boiten, J.-W., da Silva Santos, L. B., Bourne, P. E., Bouwman, J., Brookes, A. J., Clark, T., Crosas, M., Dillo,
 - I., Dumon, O., Edmunds, S., Evelo, C. T., Finkers, R., Gonzalez-Beltran, A., Gray, A. J. G., Groth, P., Goble,
- 645 C., Grethe, J. S., Heringa, J., 't Hoen, P. A. C., Hooft, R., Kuhn, T., Kok, R., Kok, J., Lusher, S. J., Martone,
- M. E., Mons, A., Packer, A. L., Persson, B., Rocca-Serra, P., Roos, M., van Schaik, R., Sansone, S.-A.,
- Schultes, E., Sengstag, T., Slater, T., Strawn, G., Swertz, M. A., Thompson, M., van der Lei, J., van Mulligen,
- E., Velterop, J., Waagmeester, A., Wittenburg, P., Wolstencroft, K., Zhao, J., and Mons, B.: The FAIR
- 649 Guiding Principles for scientific data management and stewardship, Scientific Data, 3, 160018,
- 650 https://doi.org/10.1038/sdata.2016.18, 2016.
- Zheng, J. and Suh, S.: Strategies to reduce the global carbon footprint of plastics, Nature Climate Change, 9,
- 652 374–378, https://doi.org/10.1038/s41558-019-0459-z, 2019.